

Beyond mean-field dynamics in open Bose-Hubbard chains

D. Witthaut,^{1,*} F. Trimborn,² H. Hennig,¹ G. Kordas,³ T. Geisel,¹ and S. Wimberger³

¹*Max-Planck-Institute for Dynamics and Self-Organization, D-37073 Göttingen, Germany*

²*Institut für theoretische Physik, Leibniz Universität Hannover, D-30167 Hannover, Germany*

³*Institut für theoretische Physik and Center for Quantum Dynamics,*

Universität Heidelberg, D-69120 Heidelberg, Germany

(Dated: November 3, 2018)

We investigate the effects of phase noise and particle loss on the dynamics of a Bose-Einstein condensate in an optical lattice. Starting from the many-body master equation, we discuss the applicability of generalized mean-field approximations in the presence of dissipation as well as methods to simulate quantum effects beyond mean-field by including higher-order correlation functions. It is shown that localized particle dissipation leads to surprising dynamics, as it can *suppress* decay and *restore* the coherence of a Bose-Einstein condensate. These effects can be applied to engineer coherent structures such as stable discrete breathers and dark solitons.

PACS numbers: 03.75.Lm, 03.65.Yz, 03.75.Gg

I. INTRODUCTION

Decoherence and dissipation, caused by the irreversible coupling of a quantum system to its environment, represent a major obstacle for the long-time coherent control of quantum states. However, in the last years it has been realized that dissipation can be extremely useful if it can be controlled accurately. Recent experiments have shown that strong correlations can be induced by two-body losses in ultracold quantum gases [1, 2]. Three-body losses can be tailored to generate effective three-body interactions [3] and to prepare strongly correlated states for quantum simulations of color superfluidity [4], quantum hall physics [5] or d-wave pairing [6]. Even more, dissipation can be used as a universal tool in quantum state preparation [7, 8], entanglement generation [9] and quantum information processing [10]. These concepts of controlling quantum dynamics and transport are particularly important for experiments with ultracold atoms in optical lattices, where it is possible to address the quantum system with single-site resolution [11, 12]. An even higher spatial resolution has been realized with a focussed electron beam, removing atoms one-by-one from the lattice [13, 14]. The effects of such a localized particle loss on the dynamics of a Bose-Einstein condensate (BEC) have been investigated from a nonlinear dynamics viewpoint in several papers in the last years, discussing the possibility to induce nonlinear structures such as bright breathers [15, 16], dark solitons [17] or ratchets [18]. These studies were based on a mean-field approximation, where the loss was introduced heuristically as an imaginary potential.

In this article we go beyond this approximation and investigate the quantum dynamics of ultracold atoms in a finite optical lattice with dissipation, which provides a distinguished model system for the study of open one-dimensional chains. Our analysis is based on a numer-

ical integration of the full many-body master equation and generalized mean-field methods. In section II, we present an explicit derivation of the mean-field equations of motion, which hold if the many-body state is close to a BEC, and generalize this approach to take into account higher order correlation functions [19, 20]. If particle loss is the only source of dissipation, the mean-field equations reduce to a non-hermitian Schrödinger equation applied previously [16, 17]. While such a non-hermitian description has been thoroughly studied for single particle quantum mechanics [21], the applicability to open many-body systems is an open issue.

Two important cases are studied in detail: In section III, we analyze how boundary dissipation induces localization and purifies a BEC. In section IV, we consider localized loss from a single lattice site, which creates a vacancy and leads to a fragmentation of the condensate. Remarkably, strong dissipation can suppress the decay of the condensate and a coherent dark soliton can be generated by properly engineering the dynamics. The techniques presented here can be directly applied in ongoing experiments [13, 14].

II. THE MEAN-FIELD LIMIT AND BEYOND

The coherent dynamics of ultracold atoms in optical lattices is described by the celebrated Bose-Hubbard Hamiltonian [22]

$$\hat{H} = -J \sum_j \left(\hat{a}_{j+1}^\dagger \hat{a}_j + \hat{a}_j^\dagger \hat{a}_{j+1} \right) + \frac{U}{2} \sum_j \hat{a}_j^\dagger \hat{a}_j^\dagger \hat{a}_j \hat{a}_j, \quad (1)$$

where \hat{a}_j and \hat{a}_j^\dagger are the bosonic annihilation and creation operators in mode j , J denotes the tunneling matrix element between the wells and U the interaction strength. We set $\hbar = 1$, thus measuring energy in frequency units. This model assumes that the lattice is sufficiently deep, such that the dynamics takes place in the lowest Bloch band only.

*Electronic address: witthaut@nld.ds.mpg.de

In the presence of dissipation, the dynamics is given by a master equation in Lindblad form [23],

$$\dot{\hat{\rho}} = -i[\hat{H}, \hat{\rho}] + \mathcal{L}\hat{\rho}. \quad (2)$$

Here, we are especially interested in the effects of localized particle loss, which can be implemented by an electron beam [13, 14] or by a strongly focussed resonant blast laser. Furthermore, phase noise is always present in experiments, which degrades the phase coherence between adjacent wells and heats the sample [24, 25]. These two processes are described by the Liouvillians [23, 26–28]

$$\mathcal{L}_{\text{loss}}\hat{\rho} = -\frac{1}{2} \sum_j \gamma_j \left(\hat{a}_j^\dagger \hat{a}_j \hat{\rho} + \hat{\rho} \hat{a}_j^\dagger \hat{a}_j - 2\hat{a}_j \hat{\rho} \hat{a}_j^\dagger \right), \quad (3)$$

$$\mathcal{L}_{\text{phase}}\hat{\rho} = -\frac{\kappa}{2} \sum_j \hat{n}_j^2 \hat{\rho} + \hat{\rho} \hat{n}_j^2 - 2\hat{n}_j \hat{\rho} \hat{n}_j, \quad (4)$$

where γ_j denotes the loss rate at site j and κ is the strength of the phase noise.

To derive the mean-field approximation, we start from the single particle reduced density matrix (SPDM) $\sigma_{jk} = \langle \hat{a}_j^\dagger \hat{a}_k \rangle = \text{tr}(\hat{a}_j^\dagger \hat{a}_k \hat{\rho})$ [19, 20, 29]. The equations of motion for σ_{jk} are obtained from the master equation (2),

$$\begin{aligned} i \frac{d}{dt} \sigma_{j,k} &= \text{tr} \left(\hat{a}_j^\dagger \hat{a}_k [\hat{H}, \hat{\rho}] + i \hat{a}_j^\dagger \hat{a}_k \mathcal{L}\hat{\rho} \right) \\ &= -J(\sigma_{j,k+1} + \sigma_{j,k-1} - \sigma_{j+1,k} - \sigma_{j-1,k}) \\ &\quad + U(\sigma_{kk}\sigma_{jk} + \Delta_{jkkk} - \sigma_{jj}\sigma_{jk} - \Delta_{jjjk}), \\ &\quad -i \frac{\gamma_j + \gamma_k}{2} \sigma_{j,k} - i\kappa(1 - \delta_{j,k})\sigma_{j,k}, \end{aligned} \quad (5)$$

where we have defined the covariances

$$\Delta_{jklm} = \langle \hat{a}_j^\dagger \hat{a}_k \hat{a}_l^\dagger \hat{a}_m \rangle - \langle \hat{a}_j^\dagger \hat{a}_k \rangle \langle \hat{a}_l^\dagger \hat{a}_m \rangle. \quad (6)$$

In the mean-field limit $N \rightarrow \infty$ with $g = UN$ fixed, one can neglect the variances Δ_{jklm} in Eq. (5) in order to obtain a closed set of evolution equations. This is appropriate for a pure BEC, because the variances scale only linearly with the particle number N , while the products $\sigma_{jk}\sigma_{lm}$ scale as N^2 . If phase noise can be neglected, i.e. $\kappa = 0$, the equations of motion (5) are equivalent to the non-hermitian discrete nonlinear Schrödinger equation

$$i \frac{d}{dt} \psi_k = -J(\psi_{k+1} + \psi_{k-1}) + U|\psi_k|^2 \psi_k - i \frac{\gamma_k}{2} \psi_k \quad (7)$$

by the identification $\sigma_{j,k} = \psi_j^* \psi_k$. This provides a proper derivation of the non-hermitian Schrödinger equation, which has previously been applied heuristically [15–17].

The mean-field approximation assumes a pure BEC and is strictly valid only in the limit $N \rightarrow \infty$. To describe many-body effects such as quantum correlations and the depletion of the condensate for large, but finite particle numbers, we generalize the Bogoliubov backreaction (BBR) method [19] to the dissipative case, taking into account the covariances (6) explicitly. We start with

the coherent part of the master equation, which yields the following evolution equations for the four-point functions:

$$\begin{aligned} i \frac{d}{dt} \langle \hat{a}_j^\dagger \hat{a}_m \hat{a}_k^\dagger \hat{a}_n \rangle &= \text{tr} \left(\hat{a}_j^\dagger \hat{a}_m \hat{a}_k^\dagger \hat{a}_n [\hat{H}, \hat{\rho}] \right) \\ &= (\epsilon_m + \epsilon_n - \epsilon_j - \epsilon_k) \langle \hat{a}_j^\dagger \hat{a}_m \hat{a}_k^\dagger \hat{a}_n \rangle \\ &\quad - J \langle \hat{a}_j^\dagger \hat{a}_m \hat{a}_k^\dagger \hat{a}_{n+1} + \hat{a}_j^\dagger \hat{a}_m \hat{a}_k^\dagger \hat{a}_{n-1} + \hat{a}_j^\dagger \hat{a}_{m+1} \hat{a}_k^\dagger \hat{a}_n \\ &\quad + \hat{a}_j^\dagger \hat{a}_{m-1} \hat{a}_k^\dagger \hat{a}_n - \hat{a}_{j+1}^\dagger \hat{a}_m \hat{a}_k^\dagger \hat{a}_n - \hat{a}_{j-1}^\dagger \hat{a}_{m+1} \hat{a}_k^\dagger \hat{a}_n \\ &\quad - \hat{a}_j^\dagger \hat{a}_m \hat{a}_{k+1}^\dagger \hat{a}_n - \hat{a}_j^\dagger \hat{a}_m \hat{a}_{k-1}^\dagger \hat{a}_n \rangle \\ &\quad + U \langle \hat{a}_j^\dagger \hat{a}_m \hat{n}_m \hat{a}_k^\dagger \hat{a}_n + \hat{a}_j^\dagger \hat{a}_m \hat{a}_k^\dagger \hat{a}_n \hat{n}_n \\ &\quad - \hat{n}_j \hat{a}_j^\dagger \hat{a}_m \hat{a}_k^\dagger \hat{a}_n - \hat{a}_j^\dagger \hat{a}_m \hat{n}_k \hat{a}_k^\dagger \hat{a}_n \rangle. \end{aligned} \quad (8)$$

Again, the interaction hamiltonian leads to higher-order correlation functions. To obtain a closed set of evolution equations, these function are truncated according to [20]

$$\begin{aligned} \langle \hat{a}_j^\dagger \hat{a}_m \hat{a}_k^\dagger \hat{a}_n \hat{a}_r^\dagger \hat{a}_s \rangle &\approx \langle \hat{a}_j^\dagger \hat{a}_m \hat{a}_k^\dagger \hat{a}_n \rangle \langle \hat{a}_r^\dagger \hat{a}_s \rangle \\ &\quad + \langle \hat{a}_j^\dagger \hat{a}_m \hat{a}_r^\dagger \hat{a}_s \rangle \langle \hat{a}_k^\dagger \hat{a}_n \rangle + \langle \hat{a}_k^\dagger \hat{a}_n \hat{a}_r^\dagger \hat{a}_s \rangle \langle \hat{a}_j^\dagger \hat{a}_m \rangle \\ &\quad - 2 \langle \hat{a}_j^\dagger \hat{a}_m \rangle \langle \hat{a}_k^\dagger \hat{a}_n \rangle \langle \hat{a}_r^\dagger \hat{a}_s \rangle. \end{aligned} \quad (9)$$

For a BEC, the six-point function scale as N^3 , while the error introduced by this approximation increases only linearly with N . The relative error induced by the truncation thus vanishes as $1/N^2$ with increasing particle number. Close to a pure condensate, the BBR method thus provides a better description of the many-body dynamics than the simple mean-field approximation, since it includes the dynamics of higher order methods at least approximately. Using this truncation, the coherent part of the dynamics is given by

$$\begin{aligned} i \frac{d}{dt} \Delta_{jmkn} &= \\ &-J[\Delta_{j,m,k,n+1} + \Delta_{j,m,k,n-1} + \Delta_{j,m+1,k,n} + \Delta_{j,m-1,k,n} \\ &\quad - \Delta_{j,m,k+1,n} - \Delta_{j,m,k-1,n} - \Delta_{j+1,m,k,n} - \Delta_{j-1,m,k,n}] \\ &+ U[\Delta_{mmkn}\sigma_{jm} - \Delta_{jjkn}\sigma_{jm} + \Delta_{jmn}\sigma_{kn} - \Delta_{jmk}\sigma_{kn} \\ &\quad + \Delta_{jmk}\sigma_{mm} + \sigma_{nn} - \sigma_{kk} - \sigma_{jj}]. \end{aligned} \quad (10)$$

Particle loss and dissipation affect the dynamics of the four-point functions as follows

$$\begin{aligned} \frac{d}{dt} \langle \hat{a}_j^\dagger \hat{a}_m \hat{a}_k^\dagger \hat{a}_n \rangle &= \text{tr} \left[\hat{a}_j^\dagger \hat{a}_m \hat{a}_k^\dagger \hat{a}_n \mathcal{L}\hat{\rho} \right] \\ &= -\frac{\gamma_j + \gamma_m + \gamma_k + \gamma_n}{2} \langle \hat{a}_j^\dagger \hat{a}_m \hat{a}_k^\dagger \hat{a}_n \rangle - \delta_{mk} \gamma_m \langle \hat{a}_j^\dagger \hat{a}_n \rangle \\ &\quad - \kappa(2 + \delta_{mn} + \delta_{jk} - \delta_{jm} - \delta_{jn} - \delta_{km} - \delta_{kn}) \\ &\quad \times \langle \hat{a}_j^\dagger \hat{a}_m \hat{a}_k^\dagger \hat{a}_n \rangle. \end{aligned}$$

In terms of the variances this yields

$$\begin{aligned} \frac{d}{dt} \Delta_{jmkn} &= -\frac{\gamma_j + \gamma_m + \gamma_k + \gamma_n}{2} \Delta_{jmkn} - \delta_{mk} \gamma_m \sigma_{jn} \\ &\quad - \kappa(\delta_{mn} + \delta_{jk} - \delta_{jn} - 2\delta_{km})(\Delta_{jmkn} + \sigma_{jm}\sigma_{kn}) \\ &\quad - \kappa(2 - \delta_{jm} - \delta_{kn}) \Delta_{jmkn}. \end{aligned} \quad (11)$$

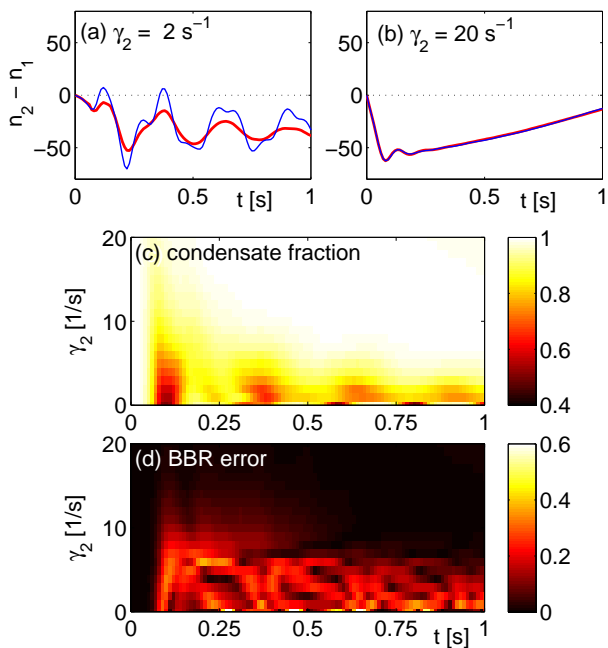


FIG. 1: (Color online) Numerical test of the BBR methods for a leaky double-well trap with loss in the second well. (a,b) Dynamics of the population imbalance $\langle \hat{n}_2 - \hat{n}_1 \rangle$ for two different values of the loss rate, comparing the BBR approximation (solid blue line) to numerically exact results (thick red line). (c) Condensate fraction λ_0/n_{tot} as a function of time and the loss rate γ_2 . (d) Trace distance (12) between the exact rescaled SPDM $\sigma(t)/n(t)$ and the respective BBR approximation. In all cases the initial state is assumed to be a pure BEC with equal population and a phase difference of π between the two modes. The remaining parameters are $J = 10 \text{ s}^{-1}$, $\kappa = 0$, $U = 0.5 \text{ s}^{-1}$ and $n(0) = 200$ atoms.

The BBR method is especially useful if the many-body state is close to, but not exactly equal to a pure BEC. In particular, it accurately predicts the onset of the depletion of the condensate mode. The number of atoms in this mode is given by the leading eigenvalue λ_0 of the SPDM $\sigma_{j,k}$, where the trace of $\sigma_{j,k}$ gives the total number of atoms n_{tot} . The ratio λ_0/n_{tot} is referred to as the condensate fraction [19, 30].

The BBR approach has been extensively tested for closed systems in [20]. Therefore, we only briefly comment on the performance of this method in the presence of dissipation. Figure 1 shows two examples of the dynamics of a BEC in a leaky double-well trap, comparing the BBR approximation (solid blue line) and numerically exact results (thick red line). The initial state is assumed to be a pure BEC with equal population and a phase difference of π between the two modes. In the case of strong dissipation, the BBR approximation predicts the correct evolution of the population imbalance $\langle \hat{n}_2 - \hat{n}_1 \rangle$ with an astonishing precision. In contrast, significant differences are observed for weak losses. This means that the presence of particle loss actually improves the performance of the BBR method, as the dissipation drives the many-

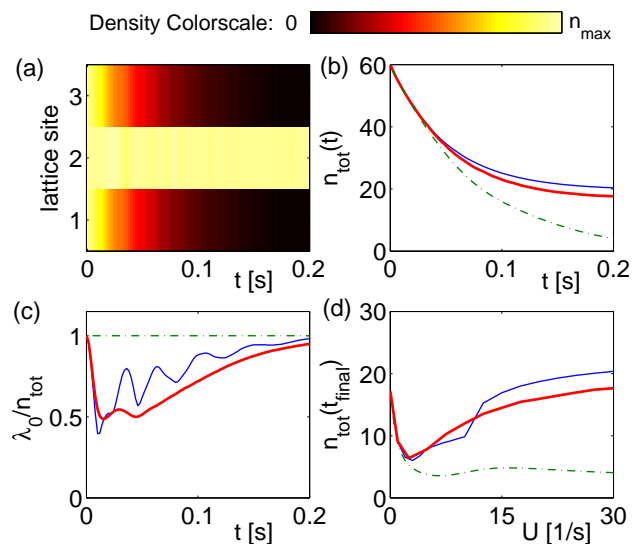


FIG. 2: (Color online) Dynamics of a BEC in a triple-well trap with boundary dissipation: (a) atomic density $\langle \hat{n}_j(t) \rangle$, (b) total particle number and (c) the condensate fraction λ_0/n_{tot} for $J = 5 \text{ s}^{-1}$, $\gamma = 20 \text{ s}^{-1}$, $\kappa = 0$, $U = 30 \text{ s}^{-1}$ and $n(0) = 60$ atoms. (d) Total particle number after a fixed propagation time $t_{\text{final}} = 0.2 \text{ s}$ as a function of the interaction strength U . Mean-field (---) and BBR (—) results are compared to numerically exact simulations with a quantum jump method averaging over 200 trajectories (thick red line).

body quantum state towards a pure BEC [36]. This is confirmed by the numerical results for the condensate fraction λ_0/n_{tot} plotted in Fig. 1 (c). A significant depletion of the condensate is only observed for small values of the loss rate γ_2 . For a further quantitative analysis of the accuracy, we compare exact and BBR results for the rescaled SPDM $\sigma(t)/n_{\text{tot}}(t)$. Figure 1 (d) shows the trace distance of the exact matrix and the matrix obtained by the BBR method,

$$d := \frac{1}{2} \text{tr}(|\sigma_{\text{BBR}}/n_{\text{BBR}} - \sigma_{\text{ex}}/n_{\text{ex}}|), \quad (12)$$

as a function of time for different values of γ_2 . For sufficiently large dissipation, one observes that the distance approximately vanishes for all times. In this regime the quantum dynamics is faithfully reproduced by the BBR approximation.

III. BOUNDARY DISSIPATION

We first analyze the effects of boundary dissipation with a focus on small systems for which numerically exact solutions of the many-particle dynamics are still possible, for instance by the quantum jump method [23, 31]. A comparison to numerically exact results for these examples provides another test of performance of the BBR approach.

We consider the decay of an initially pure, homogeneous BEC in a triple-well trap with boundary dissipation. Figure 2 (a) and (b) show the evolution of the atomic density and the total particle number for strong inter-atomic interactions $U = 30 \text{ s}^{-1}$. One observes a fast decay of the atoms at the outer sites while the population at the central site is remarkably stable. This is confirmed by the evolution of the total particle number, which rapidly drops to about one third of its initial value, where it saturates for a long time. This is a consequence of the dynamical formation of a discrete breather at the central site, which is an important generic feature of nonlinear lattices. Generally, discrete breathers, also called discrete solitons, are spatially localized, time-periodic, stable excitations in perfectly periodic discrete systems [32–35]. They arise intrinsically from the combination of nonlinearity and the discreteness of the system. In the presence of boundary dissipation, these excitations become attractively stable such that the quantum state of the atoms will converge to a pure BEC with a breather-like density for a wide class of initial states. Once a discrete breather is formed, it remains stable also if the dissipation is switched off. The crucial role of strong interactions is illustrated in Fig. 2 (d), where the residual atom number after $t_{\text{final}} = 0.2 \text{ s}$ of propagation is plotted as a function of the interaction strength. The particle number increases for large values of U to $n_{\text{tot}}(t_{\text{final}}) \approx 20$ due to the breather formation.

For strong interactions a simple mean-field approximation fails. It strongly underestimates the residual particle number as it predicts that discrete breathers are formed only for stronger losses. In contrast, the BBR results agree well with the many-particle simulation even for large values of U . We thus conclude that quantum fluctuations facilitate the formation of repulsively bound structures. Furthermore, a mean-field approach cannot account for genuine many-body features of the dynamics. Figure 2 (c) shows the evolution of the condensate fraction λ_0/n_{tot} , where λ_0 is the leading eigenvalue of the SPDM [30]. In the beginning, interactions lead to a rapid depletion of the condensate. On a longer time scale, however, dissipation restores the coherence and drives the atoms to a pure BEC localized at the central lattice site [36]. The BBR approach faithfully reproduces the depletion and re-purification but additionally predicts unphysical temporal revivals. This example thus demonstrates the strength but also the limitations of this method.

The decay dynamics of the discrete breather state is further analyzed in Fig. 3. The total atom number $n_{\text{tot}}(t)$ decreases rapidly until the discrete breather is formed at $t \approx 0.2 \text{ s}$. Afterwards the decay is much slower and clearly non-exponential. In both regimes, one can calculate the evolution of $n_{\text{tot}}(t)$ approximately, starting from the relation $\dot{n}_{\text{tot}} = -\gamma(n_1 + n_3)$. Initially, all sites are filled homogeneously, $n_1 = n_3 = n_{\text{tot}}/3$, such that the total particle number decays as

$$n_{\text{tot}}(t) \approx n_{\text{tot}}(0)e^{-2\gamma/3t}. \quad (13)$$

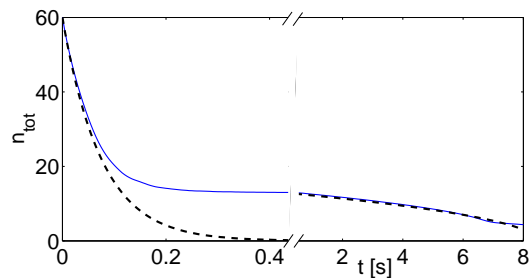


FIG. 3: (Color online) Decay of a discrete breather state for $J = 5 \text{ s}^{-1}$, $\gamma = 20 \text{ s}^{-1}$, $\kappa = 0$ and $U = 10 \text{ s}^{-1}$. Numerical results calculated with the BBR method (—) are compared to the analytic estimates (13) and (14), respectively (---).

When the discrete breather is formed, the population of the outer wells is given by $n_1 = n_3 = J^2/(U^2 n_{\text{tot}})$ in first order perturbation theory. The atom number then decays as

$$n_{\text{tot}}(t) \approx \sqrt{n_{\text{db}}^2 - 4\gamma J^2 t/U^2}, \quad (14)$$

where n_{db} is the number of atoms bound in the discrete breather state. Both approximations are compared to the BBR simulation results in Fig. 3, assuming a breather with $n_{\text{db}} = 13$ atoms. One observes an excellent agreement in the both regimes, i.e. an exponential decay for very short times ($t \lesssim 0.1 \text{ s}$) and an algebraic decay when the discrete breather is formed. The transition between the linear and nonlinear decay takes place at $t \approx 0.2 \text{ s}$. A deviation from the algebraic decay (14) for the discrete breather is observed only for very long times when the atom number is very small such that the simple perturbative estimate for $n_{1,3}$ is no longer valid.

IV. LOCALIZED LOSS

Recent experiments with ultracold atoms have demonstrated an enormous progress in spatial addressability using specialized optical imaging systems [11, 12] or a focussed electron beam [13, 14]. Especially the latter experiment allows to manipulate a Bose-Einstein condensate in an optical lattice dissipatively with single-site resolution. In the following, we study the quantum dynamics in a finite lattice of 11 sites with closed boundary conditions and loss occurring from the central site only, which leads to remarkably different decay as in the case of boundary dissipation studied above.

A remarkable feature of the quantum dynamics is illustrated in Figure 4, showing the results of a BBR simulation for an initially pure homogeneous BEC. For a modest loss rate $\gamma = 20 \text{ s}^{-1}$, atoms tunnel to the central site where they are dissipated with a rate γ , such that the BEC decays almost homogeneously. On the contrary, stronger losses ($\gamma = 100 \text{ s}^{-1}$) lead to a formation of a stable vacancy. The central site is rapidly depleted, but the

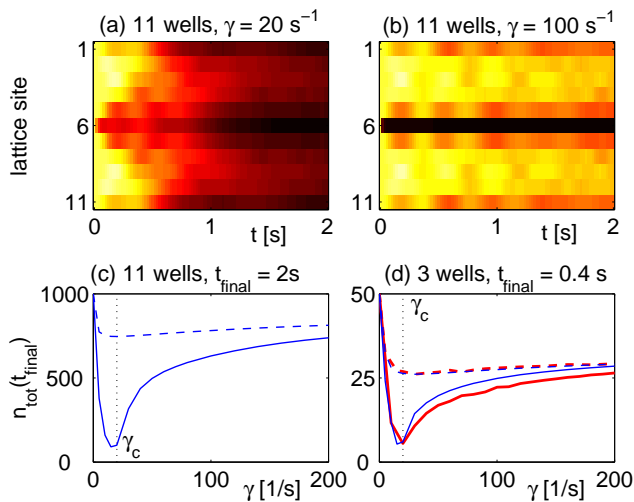


FIG. 4: (Color online) Formation of vacancies by localized loss at the central lattice site. (a,b) Evolution of the atomic density $\langle \hat{n}_j(t) \rangle$ (color scale as in Fig. 2). (c,d) Final value of the total particle number after a fixed propagation time t_{final} as a function of the loss rate γ , without (solid lines) and with strong phase noise (dashed lines, $\kappa = 50 \text{ s}^{-1}$). The remaining parameters are $J = 5 \text{ s}^{-1}$, $U = 0.2 \text{ s}^{-1}$ and $n(0) = 1000$ particles (a-c) and $U = 2 \text{ s}^{-1}$ and $n(0) = 50$ particles (d). The dynamics has been simulated with the BBR (thin blue lines) and the quantum jump method (thick red lines).

atoms in the remaining wells are mostly unaffected. Thus one faces the paradoxical situation that an increase of the loss rate can suppress the decay of the BEC. Two effects contribute to this counterintuitive behavior: (i) The absorbing potential suppresses tunneling to the leaky lattice site. This effect is present also in the linear case and can be explained by an analogy to wave optics [1]: A large mismatch of the index of refraction leads to an almost complete reflection of a wave from a surface. This is true for an imaginary index describing an absorption as well as for a real index. (ii) A dark breather stabilizes the vacancy and prevents the flow of atoms to the central site. This nonlinear structure remains stable also if the dissipation is reduced or switched off afterwards (cf. [33–35] for a discussion of the stability of breathers).

The suppressed decay of the BEC is further illustrated in Fig. 4 (c,d), where the residual atom number after a fixed propagation time is plotted as a function of the loss rate γ . The coherent output of the system, i.e. the number of lost atoms, assumes a maximum for a finite loss rate γ_c . This maximum is reminiscent of the quantum stochastic resonance discussed in [36]. In the following we will estimate the value of γ_c by determining a lower bound for γ for the dynamical breather formation. As a single (both bright and dark) breather exhibits a pronounced population imbalance between the central site and the neighboring sites, we estimate γ_c by matching the timescales of dissipation $\tau_D = 2/\gamma$ and tunneling τ_J , i.e., $\tau_D = \tau_J$. For smaller values of γ , atoms can tunnel away from the leaky lattice site again before they are

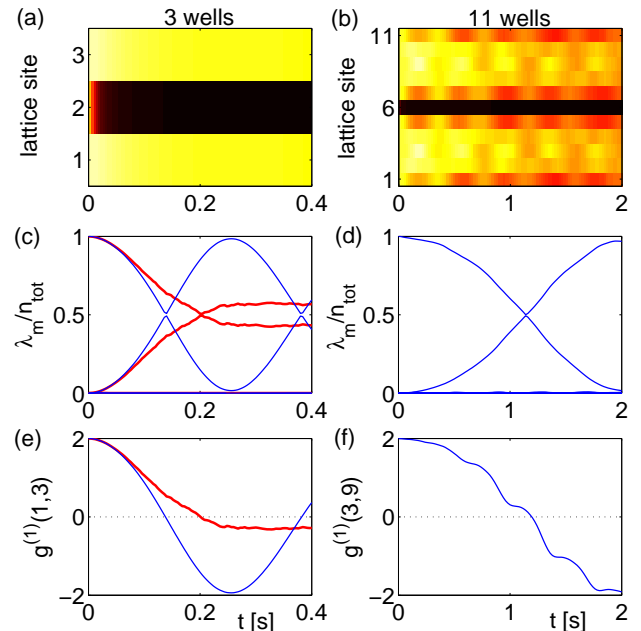


FIG. 5: (Color online) Coherence of a vacancy generated by loss from the central site: (a,b) atomic density, (c,d) scaled eigenvalues λ_m/n_{tot} of the SPDM and (e,f) phase coherence $g^{(1)}$ between the two BEC fragments. Parameters are the same as in Fig. 4 with $\gamma = 100 \text{ s}^{-1}$ and $\kappa = 0$. Results of a quantum jump simulation are plotted as thick red lines, BBR results as thin blue lines.

lost, while for larger values of γ a population imbalance can form. From Eq. (7) we read $\tau_J = 1/(2J)$ where the factor $1/2$ accounts for atoms tunneling from two sites to the leaky site. Hence, the critical loss rate is estimated as $\gamma_c = 4J$. We find good agreement of our qualitative estimate for γ_c (dotted vertical lines in Fig. 4 (c,d)) with the dip in the total particle number. An important quantity for the breather formation and stability is the effective nonlinearity of the system $\lambda = Un_{\text{tot}}(t)/2J$, which, due to particle loss, is time-dependent. Strikingly, though λ depends on the interaction strength U (which is different in Fig. 4 (c) and (d)), the fairly good estimate γ_c is independent of U .

Figure 4 (d) shows the respective results for a triple-well trap with loss from the central site. A comparison of the BBR approximation to a numerically exact many-particle simulation shows a good agreement for all values of γ . Phase noise suppresses decay as it effectively decouples the lattice sites. Thus, only the atoms initially loaded at the leaky lattice site decay as $e^{-\gamma t}$, while the other atoms remain at their initial positions. With increasing loss rate γ , the number of atoms lost from the trap approaches $\approx n(0)/M$ as shown in Fig. 4 (c,d).

The previous reasoning suggests to use dissipation as a tool to coherently engineer the quantum state of a BEC in an optical lattice. Mean-field theory predicts that dissipation can be used to efficiently create a coherent dark soliton [17], but cannot assert the coherence of the final

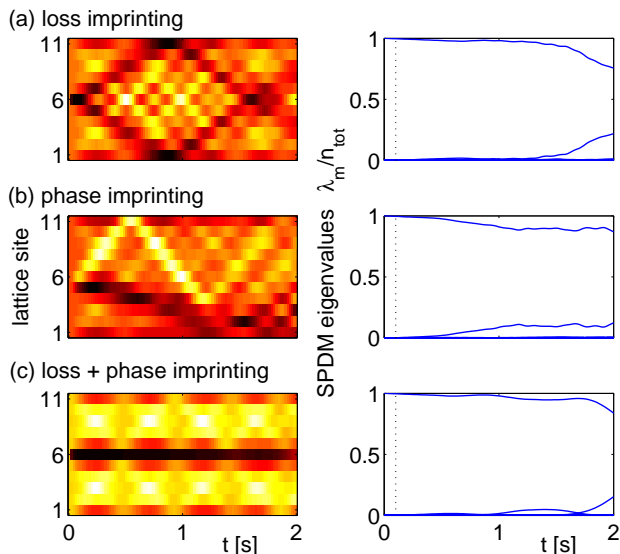


FIG. 6: (Color online) Generation of dark solitons using loss imprinting at a rate $\gamma = 100 \text{ s}^{-1}$ at the central site (a,c) and phase imprinting in the lower half of the lattice (b,c), both for times $t < 0.1 \text{ s}$ only. Shown are the atomic density (left, colorscale as in Fig. 2) and the scaled eigenvalues of the SPDM (right) calculated with the BBR method. Parameters are $J = 5 \text{ s}^{-1}$, $U = 0.1 \text{ s}^{-1}$, $\kappa = 0$ and $n(0) = 1000$ particles.

state as discussed above. The results of a BBR and a quantum jump simulation of the many-body dynamics shown in Fig. 5 reveal the limitations of the phase coherence of a soliton generated by local dissipation. The upper panels (a,b) show the rescaled eigenvalues λ_m/n_{tot} of the SPDM [30]. One observes that there are two macroscopic eigenvalues approaching $1/2$, while all remaining eigenvalues vanish approximately. This proves that the dissipation generates a fragmented BEC consisting of two incoherent parts rather than a single BEC with a solitonic wavefunction. The BBR simulations correctly describe the fragmentation of the condensate, but predict temporal revivals of the coherence which must be considered as artifacts of the approximation. Experimentally, one can test the coherence by the interference of the two fragments in a time-of-flight measurement. Figure 5 (e,f) shows the coherence

$$g^{(1)}(\ell, m) = \frac{\langle \hat{a}_\ell^\dagger \hat{a}_m + a_m^\dagger \hat{a}_\ell \rangle}{\sqrt{\langle \hat{n}_\ell \rangle \langle \hat{n}_m \rangle}} \quad (15)$$

between the wells ℓ and m . One clearly observes the breakdown of phase coherence between the two condensate fragments.

In order to overcome the loss of coherence, one can, however, engineer the many-body dynamics. Figure 6 illustrates the generation of dark solitons comparing three different strategies. If the dissipation is switched off after the generation of a vacancy at $t = 0.1 \text{ s}$, the condensate remains pure for long times. However, the vacancy is not stable but decays into two dark solitons traveling out-

wards [17], where they are reflected at the boundaries. The effects of a phase imprinting, which is an established experimental method [37], are shown in Fig. 6 (b). A local potential is applied to the lower half of the lattice for $t < 0.1 \text{ s}$ imprinting a phase difference of π . Again coherence is preserved but the generated solitons travel outwards. A coherent and stable dark soliton can be engineered by combining both methods, as shown in Fig. 6 (c). The generated dark soliton stays at its initial position and remains coherent over a long time.

V. CONCLUSION

We have discussed the influence of localized particle dissipation on the dynamics of a finite one-dimensional Bose-Hubbard chain, which describes a Bose-Einstein condensate in a deep optical lattice [13, 14]. Starting from the many-body master equation, we have derived the mean-field approximation and the dissipative Bogoliubov backreaction method, which allows a consistent calculation of the depletion of the condensate.

Two important special cases have been studied in detail. Particle loss at the *boundary* leads to localization and the formation of coherent discrete breathers. Surprisingly, dissipation together with interactions can repurify a BEC. A striking effect of *localized loss* is that strong dissipation can effectively *suppress* decay and induce stable vacancies. The decay shows a pronounced maximum for intermediate values of the loss rate, when the timescales of the dissipation and the tunneling are matched. Combined with an external potential, these effects can be used to generate stable coherent dark solitons. These examples show that engineering the dissipation is a promising approach for controlling the dynamics in complex quantum many-body systems.

Ultracold atoms provide a distinguished model system for the dynamics of interacting quantum systems, such that the effects discussed in the present paper may be observed in different systems, too. In particular, quantum transport of single excitations driven by *local* dissipation has recently been studied in a variety of physical systems ranging from spin chains [38] to light-harvesting biomolecules [39]. On the other hand, it has also been shown on the mean-field level that nonlinear excitations such as discrete breathers play an important role for quantum transport in these systems (cf. [33, 34, 40] and references therein). Thus it is of general interest to further explore the regime which interpolates between the nonlinear mean-field dynamics and the many-body quantum dynamics in the spirit of the work presented here.

Acknowledgments

We thank T. Pohl for helpful comments and M. K. Oberthaler for stimulating discussions and ideas on experimental possibilities. We acknowledge financial sup-

port by the Deutsche Forschungsgemeinschaft (DFG) via the Forschergruppe 760 (grant number WI 3426/3-1), the Heidelberg Graduate School of Fundamental Physics

(grant number GSC 129/1) and the research fellowship programme (grant number WI 3415/1-1), as well as the Studienstiftung des deutschen Volkes.

-
- [1] N. Syassen, D. M. Bauer, M. Lettner, T. Volz, D. Dietze, J. J. Garcia-Ripoll, J. I. Cirac, G. Rempe, and S. Dürr, *Science* **320**, 1329 (2008).
- [2] J. J. Garcia-Ripoll, S. Dürr, N. Syassen, D. M. Bauer, M. Lettner, G. Rempe, and J. I. Cirac, *New J. Phys.* **11**, 013053 (2009).
- [3] A. J. Daley, J. M. Taylor, S. Diehl, M. Baranov, and P. Zoller, *Phys. Rev. Lett.* **102**, 040402 (2009).
- [4] A. Kantian, M. Dalmonte, S. Diehl, W. Hofstetter, P. Zoller, and A. J. Daley, *Phys. Rev. Lett.* **103**, 240401 (2009).
- [5] M. Roncaglia, M. Rizzi, and J. I. Cirac, *Phys. Rev. Lett.* **104**, 096803 (2010).
- [6] S. Diehl, W. Yi, A. J. Daley, P. Zoller, arXiv:1007.3420v1
- [7] S. Diehl, A. Micheli, A. Kantian, B. Kraus, H. P. Büchler, and P. Zoller, *Nature Physics* **4**, 878 (2008).
- [8] B. Kraus, H. P. Büchler, S. Diehl, A. Kantian, A. Micheli, and P. Zoller, *Phys. Rev. A* **78**, 042307 (2008).
- [9] H. Krauter, C. A. Muschik, K. Jensen, W. Wasilewski, J. M. Petersen, J. I. Cirac, and E. S. Polzik, arXiv:1006.4344.
- [10] F. Verstraete, M. M. Wolf, and J. I. Cirac, *Nature Physics* **5**, 633 (2009).
- [11] W. S. Bakr, J. I. Gillen, A. Peng, S. Fölling, and M. Greiner, *Nature* **462**, 74 (2009).
- [12] J. F. Sherson, C. Weitenberg, M. Endres, M. Cheneau, I. Bloch, and S. Kuhr, *Nature* **467**, 68 (2010).
- [13] T. Gericke, P. Würtz, D. Reitz, T. Langen, and H. Ott, *Nature Physics* **4**, 949 (2008).
- [14] P. Würtz, T. Langen, T. Gericke, A. Koglbauer, and H. Ott, *Phys. Rev. Lett.* **103**, 080404 (2009).
- [15] R. Livi, R. Franzosi, and G.-L. Oppo, *Phys. Rev. Lett.* **97**, 060401 (2006).
- [16] G. S. Ng, H. Hennig, R. Fleischmann, T. Kottos, and T. Geisel, *New J. Phys.* **11**, 073045 (2009).
- [17] V. A. Brazhnyi, V. V. Konotop, V. M. Perez-Garcia, and H. Ott, *Phys. Rev. Lett.* **102**, 144101 (2009).
- [18] G. G. Carlo, G. Benenti, G. Casati, S. Wimberger, O. Morsch, R. Mannella, and E. Arimondo, *Phys. Rev. A* **74**, 033617 (2006).
- [19] A. Vardi and J. R. Anglin, *Phys. Rev. Lett.* **86**, 568 (2001), J. R. Anglin and A. Vardi, *Phys. Rev. A* **64**, 013605 (2001).
- [20] I. Tikhonenkov, J. R. Anglin, and A. Vardi, *Phys. Rev. A* **75**, 013613 (2007).
- [21] Y. V. Fyodorov, D. V. Savin, and H.-J. Sommers, *J. Phys. A.* **38**, 10731 (2005).
- [22] D. Jaksch, C. Bruder, J. I. Cirac, C. W. Gardiner, and P. Zoller, *Phys. Rev. Lett.* **81**, 3108 (1998).
- [23] H.-P. Breuer and F. Petruccione, *The theory of open quantum systems*, Oxford University Press (2002).
- [24] R. Gati, B. Hemmerling, J. Fölling, M. Albiez, and M. K. Oberthaler, *Phys. Rev. Lett.* **96**, 130404 (2006).
- [25] F. Trimborn, D. Witthaut, and H. J. Korsch, *Phys. Rev. A* **77**, 043631 (2008); *Phys. Rev. A* **79**, 013608 (2009).
- [26] J. R. Anglin, *Phys. Rev. Lett.* **79**, 6 (1997).
- [27] J. Ruostekoski and D. F. Walls, *Phys. Rev. A* **58**, R50 (1998).
- [28] H. Pichler, A. J. Daley, and P. Zoller, *Phys. Rev. A* **82**, 063605 (2010).
- [29] F. Trimborn, D. Witthaut, and S. Wimberger, *J. Phys. B: At. Mol. Opt. Phys.* **41**, 171001 (FTC) (2008).
- [30] A. J. Leggett, *Rev. Mod. Phys.* **73**, 307 (2001).
- [31] J. Dalibard, Y. Castin, and K. Mølmer, *Phys. Rev. Lett.* **68**, 580 (1992).
- [32] A. Trombettoni and A. Smerzi, *Phys. Rev. Lett.* **86**, 2353 (2001).
- [33] D. K. Campbell, S. Flach, and Y. S. Kivshar, *Phys. Today*, **57**, 43 (2004).
- [34] S. Flach and A. Gorbach, *Phys. Rep.* **467**, 1 (2008).
- [35] H. Hennig, J. Dorignac, D. K. Campbell, *Phys. Rev. A* **82**, 053604 (2010).
- [36] D. Witthaut, F. Trimborn, and S. Wimberger, *Phys. Rev. Lett.* **101**, 200402 (2008); *Phys. Rev. A* **79**, 033621 (2009).
- [37] J. Denschlag, J. E. Simsarian, D. L. Feder, C. W. Clark, L. A. Collins, J. Cubizolles, L. Deng, E. W. Hagley, K. Helmerson, W. P. Reinhardt, S. L. Rolston, B. I. Schneider, and W. D. Phillips, *Science* **287**, 97 (2000).
- [38] S. R. Clark, J. Prior, M. J. Hartmann, D. Jaksch, and M. B. Plenio, *New J. Phys.* **12**, 025005 (2010).
- [39] M. Sarovar, A. Ishizaki, G. R. Fleming, and K. B. Whaley, *Nature Phys.* **6**, 462 (2010).
- [40] Y. Zolotaryuk, S. Flach, and V. Fleurov, *Phys. Rev. B* **63**, 214422 (2001).